FULL PAPER

Dalton
www.rsc.org/dalton

Novel topologies in Ni^{II} cluster chemistry: Incorporation of alkaline-earth metals in the new $[Ni^{II}_6Mg^{II}_2]$ and $[Ni^{II}_8M^{II}]$ (M = Sr, Ba) cages †

Guillem Aromí,*[a] Olivier Roubeau,[b] Madeleine Helliwell,[a] Simon J. Teat[c] and Richard E. P. Winpenny *[a]

[a] *Department of Chemistry, The University of Manchester, Oxford Road, Manchester, UK M13 9PL. E-mail: richard.winpenny@man.ac.uk; Fax: +44-161-275-4654; Tel: +44-161-275-4616*

[b] *Centre de Recherche Paul Pascal, 115 avenue du Dr Schweitzer, 33600 Pessac, France*

[c] *CCLRC Daresbury Laboratory, Warrington, Cheshire, UK WA4 4AD*

Received 29th April 2003, Accepted 2nd July 2003
First published as an Advance Article on the web 18th July 2003

The reaction of the complex $[Ni_2(H_2O)(piv)_4(Hpiv)_4]$ (**1**) (Hpiv = pivalic acid) with Hppo (3-phenylpyrazolin-5-one) in the presence of a base of an alkaline-earth metal (M^{II} = Mg^{II}, Sr^{II} or Ba^{II}) has led to three different Ni^{II} clusters whose structures are controlled by the nature of M^{II}. The formulae of the new heteronuclear cages are $[Ni_6Mg_2(OH)_2(ppo)_4(piv)_{10}(Hppo)_4(MeOH)_2]$ (**2**), $[Ni_8Sr(OH)_2(ppo)_6(piv)_{10}(Hppo)_5(Hpiv)_2(MeCN)]$ (**3**) and $[Ni_8Ba(OH)_2(ppo)_6(piv)_{10}(Hppo)_{5.3}(Hpiv)_{0.7}(MeCN)_2]$ (**4**). Magnetic measurements indicate that the spin ground state of **2** consists of two independent $S = 3$ units, while the presence of two non-interacting $S = 2$ fragments in the molecule is postulated for compounds **3** and **4**.

Introduction

Among the main driving forces fuelling the development of synthetic coordination chemistry for the preparation of novel polynuclear complexes[1] is the discipline of molecular magnetism. Some discrete aggregates of open-shell 3d metals display unusually high spin ground states, *S*,[2–5] and these rare species were originally perceived as potential building blocks for the preparation of molecule-based magnets.[6] This area of research received renewed impetus with the discovery of single-molecule magnets (SMM's).[7,8] Such molecules are capable of retaining the orientation of their spin magnetic moment at low temperatures, which turns them into potential memory storage devices. It is established now that the presence of a high *S* value and large magnetoanisotropy, as gauged by the zero field splitting (ZFS) parameter *D*, are necessary conditions for a molecule to show this behaviour.[9] Many efforts in synthetic coordination chemistry are now aimed at producing new systems with improved properties such that these phenomena can be observed at higher temperatures.

There are two contrasting approaches to produce high-spin transition metal clusters; the first can be termed "rational molecular design" and the second the "serendipitous approach". The first method relies on the precise knowledge on the manner in which the species of a reaction system will interact, in such a way that the final structure of the ensuing clusters can be predicted. This has been achieved for example following a stepwise synthetic method by means of linear bridging ligands such as CN^-, and metals with a precise coordination geometry, using capping ligands to prevent infinite growth. Thus, a large number of cyanide-based spin clusters have been prepared in this manner.[10] Another strategy within the framework of this approach is the design and preparation of polynucleating ligands where the binding sites are distributed in such a manner that a number of transition metals are assembled into molecular species with a precise topology.[11,12] The second method in the synthesis of polynuclear transition metal clusters makes use of ligands that can bridge metals in a variety of orientations and binding modes, so that a large number of structural outcomes are possible. The identity of the final products, however, is very difficult to predict. Carboxylates, most often in combination with oxide or hydroxide groups, have proven extremely productive in this respect,[13–17] but many other ligands have also been used.[4,18–20] In this context, the exploration of new families of bridging ligands remains important in order to access novel topologies within this field of chemistry.

We have recently started a program aimed at the investigation of the coordination properties of the family of polydentate, bridging ligands constituted by the pyrazolinoles (Hpz, see Scheme 1). These can be prepared in a number of derivatives (R = Ph, Hppo; Me, Hmpo; Et, Hepo; CF_3; Hfpo). The first results have proven extremely encouraging, with the serendipitous preparation of the largest Ni^{II} cyclic aggregate, a $[Ni_{24}]$ wheel,[21] or the first $[Mn_{14}]$ cluster produced to that date[22] (another such example has appeared recently in the literature since then).[23] In exploring the reactivity of this type of ligand with the Ni^{II}/piv^- reaction system (Hpiv = pivalic or *tert*-butanoic acid), Na^I, arising from the base used during the reaction was found as a part of the molecule of the final product. This led to a comprehensive study where all suitable M^I ions from Group 1 in the Periodic Table were scanned, in order to establish whether the nature of the alkali metal had an influence on the structure of the resulting complex.[24] The results from such investigation showed that, in some instances, this was indeed the case, this being ascribed to small changes in stability involved with the variation of the atomic radius of M^I. Thus, a number of complexes in a rich variety of architectures were obtained, incorporating Li^I, Na^I, K^I, Rb^I or Cs^I, with nuclearities ranging from $[Ni^{II}_4Na^I_4]$, $[Ni^{II}_5Na^I_4]$, $[Ni^{II}_5Li^I_6]$ and $[Ni^{II}_8M^I_2]$ (M = K, Rb, Cs). Such a family of compounds affords the possibility of a systematic study on the influence that various

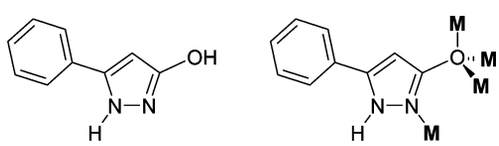

Scheme 1 Hppo (left) and ppo in its 4.31 coordination mode (right).

† Electronic supplementary information (ESI) available: Fig. S1. PLATON representation of $[Ni_8Sr(OH)_2(ppo)_6(piv)_{10}(Hppo)_5(Hpiv)_2(MeCN)]$ (**3**). See http://www.rsc.org/suppdata/dt/b3/b304713j/

DOI: 10.1039/b304713j

geometric or chemical factors have on the intramolecular magnetic exchange within Ni^{II}/piv^{-} clusters.

In this paper, we report on the extension of this concept to the group of alkaline-earth metals. The change of cationic charge from +1 to +2 was expected to have an even more profound impact on the final structure. Also, it was hoped that similar effects as seen for Group 1 would be observed in moving down Group 2.

Experimental

Synthesis

All reagents were used as received except otherwise indicated. The mixture $[Mg(OMe)_2 \cdot Mg(OH)_2]$ was obtained as a white powder by refluxing Mg metal in MeOH for two days, in air, and removing the solvent under reduced pressure. The composition was determined by elemental analysis. The ligand 3-phenylpyrazolin-5-one (Hppo) was synthesized as described in the literature.[22] The dimer $[Ni_2(H_2O)(piv)_4(Hpiv)_4]$ (**1**) was prepared as reported elsewhere.[25]

$[Ni_6Mg_2(OH)_2(ppo)_4(piv)_{10}(Hppo)_4(MeOH)_2]$ (2). To a solution of **1** (600 mg, 0.63 mmol) in MeOH (20 mL) was added a slurry of Hppo (202 mg, 1.26 mmol) and the basic mixture $[Mg(OH)_2Mg(OMe)_2]$ (55 mg, 0.76 mmol of Mg^{II}) in MeOH (20 ml). The green cloudy solution was stirred for 3 days, after which it was rotaevaporated to obtain a green oil. This oil was extracted with MeCN (20 mL) and the mixture was filtered. The filtrate was left unperturbed for a few days and green crystals of the product, suitable for X-ray diffraction, were collected by filtration in 37% yield. The complex was found to exchange the MeOH terminal ligands by H_2O molecules upon exposure to air to form $[Ni_6Mg_2(OH)_2(ppo)_4(piv)_{10}(Hppo)_4(H_2O)_2]$ (**2a**). Anal. Calc. (Found) for **2a**·MeCN: C, 53.18 (52.85); H, 5.72 (5.83); N, 8.50 (8.77).

$[Ni_8Sr(OH)_2(ppo)_6(piv)_{10}(Hppo)_5(Hpiv)_2(MeCN)]$ (3) and $[Ni_8Ba(OH)_2(ppo)_6(piv)_{10}(Hppo)_{5.3}(Hpiv)_{0.7}(MeCN)_2]$ (4). Complexes **3** and **4** were synthesized in the same manner, using the appropriate source of alkaline-earth ion, respectively. The preparation of these is given in the **3/4** format. To a solution of **1** (600 mg, 0.63 mmol) in MeOH (20 mL) was added a slurry of Hppo (303 mg, 1.89 mmol) and $Sr(OH)_2/Ba(OH)_2 \cdot H_2O$ (20/30 mg, 0.16 mmol) in MeOH (20 ml). The green cloudy solution became transparent and it was stirred for 5 h, after which it was rotaevaporated to obtain a green crude product. This crude product was extracted with MeCN (20 mL) and the mixture was filtered. The filtrate was left to stand and green crystals formed within hours. After a week, the crystals, which were suitable for X-ray crystallography, were collected by filtration and dried in air. The yield was 89/92%. Anal. Calc. (Found) for **3**: C, 53.66 (53.51); H, 5.51 (5.52); N, 8.94 (9.07). Compound **4** was found to exchange the MeCN terminal ligands by H_2O molecules upon air exposure to yield $[Ni_8Ba(OH)_2(ppo)_6(piv)_{10}(Hppo)_{5.3}(Hpiv)_{0.7}(H_2O)_2]$ (**4a**). Anal. Calc. (Found) for **4a**: C, 52.31 (52.23); H, 5.30 (5.09); N, 8.88 (8.69).

Crystallography

Data were collected on a Bruker SMART APEX CCD diffractometer (Mo-Kα, $\lambda = 0.71073$ Å) (**2** and **3**) or a Bruker SMART 1K CCD diffractometer (synchrotron, $\lambda = 0.6869$ Å) (**4**). The selected crystals were mounted within a plastic cryoloop (**2** and **3**) or on the end of a piece of glass wool (**4**) using Flombin oil and placed in the cold flow produced with an Oxford Cryosystems 700 Series Cryostream cooler (100 K, **2** and **3**) or an Oxford cryosystems 600 series cryostream cooler (150 K, **4**). Complete hemispheres of data were collected using ω-scans (0.3° (**2** and **3**) or 0.2° (**4**); 30 (**2** and **3**) or 1 (**4**) s $frame^{-1}$). Integrated intensities were obtained with SAINT+ [26] and (for **3**) they were corrected for absorption using SADABS. No absorption correction was made for **2** and **4**. Structure solution and refinement was performed with the SHELXTL-package.[26] All the structures were solved by direct methods and completed by iterative cycles of ΔF syntheses and full-matrix least-squares refinement against F^2. The number of parameters used were 878, 499 restraints (**2**), 2294, 1442 restraints (**3**) and 1948, 1518 restraints (**4**). Two groups of Me C-atoms of complex **2** (C31–C33 and C57–C62) were disordered over 2 sites each, whose occupancies were constrained to sum to 1.0. The components of the disordered phenyl ring (C57–C67) were constrained to be regular hexagons. All non-H atoms were refined anisotropically, except those of the disordered phenyl ring. H atoms were included in calculated positions.

In complex **3**, three phenyl rings were disordered over two sites, whose occupancies were constrained to sum to 1.0, as were the Me C-atoms of a *t*-Bu group. One Hpiv group (O35–C152) was poorly ordered and its geometry was restrained to be the same as for the other one (O33–C147). Most non-H atoms were refined anisotropically, except for some of the disordered or partially occupied atoms. H atoms were included in calculated positions.

All non-H atoms of complex **4** were found in the difference map and were refined anistropically, except for the disordered groups and solvent molecules. Geometrical and displacement parameters restraints were used to model the disordered groups. All hydrogen atoms were placed geometrically or in the best position to form a good hydrogen bond where possible, except for some methyl groups attached to non-tetrahedral carbons. In these cases the hydrogen could not be located and were therefore left out of the refinement. Analysis of the bonding of the two ppo ligands bound to the Ba atom through O indicates that these are hydroxyls and that these ppo ligands are in fact Hppo and neutral. However, these hydrogen atoms could not be found or put in calculated positions and were therefore omitted from the refinement. The hydrogen atoms were refined using a riding model.

CCDC reference numbers 208978–208980 (**2**–**4**).

See http://www.rsc.org/suppdata/dt/b3/b304713j/ for crystallographic data in CIF or other electronic format.

Physical measurements

FT-IR spectra were collected on a Perkin Elmer Spectrum RXI spectrometer. Elemental analysis was performed in house with a Carlo Erba Instruments CHNS-O EA-1108 Elemental Analyzer. Field cooled measurements of the magnetisation of smoothly powdered microcrystalline samples of (**2a**, 30.15 mg), (**3**, 27.88 mg) and (**4a**, 24.61 mg) were performed in the range 300–1.8 K with a Quantum Design MPMS-7XL SQUID magnetometer with an applied field of 1 or 10 kG. Corrections for diamagnetic contributions of the sample holder to the measured magnetization and of the sample to the magnetic susceptibility were performed experimentally or by using Pascal's constants, respectively.

Results and discussion

Synthesis

In previous work, we have demonstrated the feasability of influencing the nuclearity and structure of Ni^{II} clusters by changing the nature of the alkali ion of the base used during the reaction. Thus, reactions involving all suitable cations from Group 1 of the Periodic Table (Li^{I}, Na^{I}, K^{I}, Rb^{I} and Cs^{I}) gave access to a large family of Ni^{II} aggregates with four different nuclearities, which included the alkali metal in the structure.[24] The source of Ni^{II} in this work was the pivalate bridged dinuclear complex $[Ni_2(H_2O)(piv)_4(Hpiv)_4]$ (**1**),[25] while various pyrazolinol derivatives were used as polynucleating ligands. In view of these results, efforts to create a second generation of

such compounds by incorporating alkaline-earth cations were initiated. Thus, the reaction in methanol of **1** with 3-phenylpyrazolin-5-one (Hppo) in the presence of Mg^{II} (in form of $[Mg(OMe)_2{\cdot}Mg(OH)_2]$) led to a crude oil after evaporation of the solvent, which, upon extraction with MeCN, produced crystals of the heterometallic cluster $[Ni_6Mg_2(OH)_2(ppo)_4(piv)_{10}(Hppo)_4(MeOH)_2]$ (**2**). This transformation can be described with the balanced equation below (eqn. (1)).

$$3\,[Ni_2(H_2O)(piv)_4(Hpiv)_4] + Mg(OMe)_2{\cdot}Mg(OH)_2 + 8\,Hppo \longrightarrow [Ni_6Mg_2(OH)_2(ppo)_4(piv)_{10}(Hppo)_4(MeOH)_2] + 14\,Hpiv + 3\,H_2O \quad (1)$$

Complex **2**, represents a new addition to the series of existing Ni^{II}/piv/pz complexes. It is the first incorporating a cation from Group 2, and its structure (*vide infra*) is unprecedented. Interestingly, it was not possible to isolate any product by using $Mg(OH)_2$ as base, presumably because of the insolubility of the latter in this reaction system.

Following the same principle as previously for the alkali metals, the reaction that produced **2** was performed with other Group 2 metals. Hence, the analogous method employing $Sr(OH)_2$ led to the preparation of $[Ni_8Sr(OH)_2(ppo)_6(piv)_{10}(Hppo)_5(Hpiv)_2(MeCN)]$ (**3**). A balanced equation for this reaction can be written as in eqn. (2).

$$4\,[Ni_2(H_2O)(piv)_4(Hpiv)_4] + Sr(OH)_2 + 11\,Hppo + MeCN \longrightarrow [Ni_8Sr(OH)_2(ppo)_6(piv)_{10}(Hppo)_5(Hpiv)_2(MeCN)] + 4\,H_2O + 20\,Hpiv \quad (2)$$

As for some of the Group 1 cations, changing from Mg^{II} to Sr^{II} resulted in a dramatic change of structure of the final product (*vide infra*). The reaction using $Ba(OH)_2$, however, delivered the related complex $[Ni_8Ba(OH)_2(ppo)_6(piv)_{10}(Hppo)_{5.3}(Hpiv)_{0.7}(MeCN)_2]$ (**4**). This cluster is the Ba^{II} analogue of **3**, differing only in the nature of some terminal ligands. An equation similar to eqn. (2) can be written to describe the transformation leading to **4**. The thermodynamic stability of **3** and **4** is reflected in the fact that almost quantitative yields were obtained when close to stoichiometric amounts were employed for the synthesis.

The influence of Ca^{II} in this reaction system was investigated by using $Ca(OMe)_2$ as a base. The same procedure as for the previous reactions yielded small needles of a green product containing the same set of ligands as **2**, **3** and **4**, as assessed by IR spectroscopy. The presence of Ca^{II} in this solid was confirmed by elemental analysis. The nature of this product could not be established, since crystals suitable for X-ray diffraction have not been obtained.

Description of structures

The structure of complexes **2**, **3** and **4** are represented in Figs. 1–3, 5 and 7. Ranges of selected interatomic distances are given in the captions of these figures. Crystallographic data for these complexes are listed in Table 1 while metric parameters of the cores are listed in Tables 2 and 3.

$[Ni_6Mg_2(OH)_2(ppo)_4(piv)_{10}(Hppo)_4(MeOH)_2]$ (2). The core of **2** (Figs. 1 and 5) consists of two μ_3-hydroxo centered Ni^{II} triangles which are related by a center of symmetry and are linked to each other through a central $[Mg^{II}_2O_2]$ unit. By virtue of the crystallographic symmetry, these two triangles lie on rigorously parallel planes, each of them forming an angle of 84.36(1)° with the idealized plane of the $[Mg^{II}_2O_2]$ moiety. In each triangle, two edges are capped by one μ-carboxylate each, bridging Ni2 to Ni1 and Ni3, respectively. The third edge is capped by the oxygen atom of a ppo ligand, which besides Ni1 and Ni3, is bound to one Mg^{II} center. This ligand is also linked to Ni2 *via* the α-N donor of the pyrazole ring (the coordination mode of this ligand being therefore 4.31, in Harris notation).[27] Each $[Ni^{II}_3]$ unit is bridged further to the central magnesium ions through one more ppo ligand (in the 3.21 coordination mode, *via* Ni1), one μ_3-pivalate (*via* Ni1 and Ni3) and one additional μ-pivalate (*via* Ni3). The distorted octahedral coordination around Ni^{II} in each triangle is completed by two terminal Hppo molecules (bound through their α-nitrogen atom to Ni1 and Ni2, respectively), one molecule of methanol (bound to Ni2) and one terminal pivalate group (attached to Ni1). The latter ligand is forming a hydrogen bond with the central μ_3-OH^- group (O–H ··· O distance, 2.716 Å). The Mg^{II} ions are in a pentacoordinated environment that lies approximately halfway between square pyramidal and trigonal bipyramidal (τ = 0.4, where τ is 0 and 1 for the perfect square-pyramidal and trigonal-bipyramidal geometries, respectively).[28] There are two types of intermetallic distances within the $[Ni^{II}_3]$ units, one short (Ni1 ··· Ni3, 2.8406(11) Å) and two long (Ni1 ··· Ni2, 3.3616(9) and Ni2 ··· Ni3, 3.454(1) Å). This is because the Ni1 ··· Ni3 pair is bridged by two single O atoms (from piv^- and ppo^-, respectively) in addition to the central μ_3-OH^- ligand, compared to one didentate *syn*,*syn*-pivalate group for each of the other two pairs. The Mg ··· Mg distance is 3.160(3) Å. In examining the packing of the molecules in the crystal, no intermolecular H-bonding interactions were found. Despite the presence of numerous aromatic rings in **2**, the presence of π–π stacking between clusters was not observed. The only mechanism of inter-cluster interaction that could be identified was of the C–H ··· π-ring type. Therefeore, the clusters in the solid state are magnetically well isolated, the shortest inter-cluster Ni ··· Ni distance being 9.997 Å.

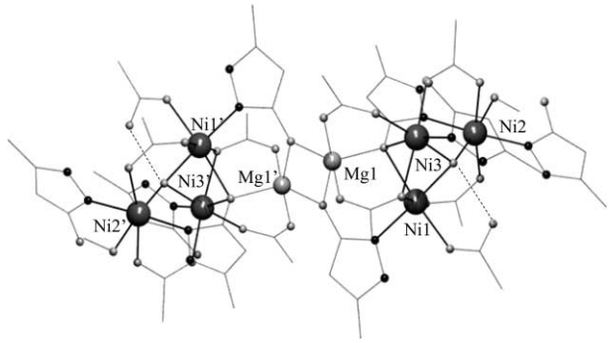

Fig. 1 Povray representation of $[Ni_6Mg_2(OH)_2(ppo)_4(piv)_{10}(Hppo)_4(MeOH)_2]$ (**2**). Only the *ipso*-C atoms of ppo or Hppo are shown. The CH_3 groups of piv^- and hydrogen atoms have been removed for clarity. Dashed lines are H-bondings. Code for unlabelled atoms: grey, O; black, N; rest, C. Interatomic distance ranges [Å]: Ni–O(OH), 1.985–2.009; Ni–O(ppo), 2.204–2.216; Ni–O(piv), 2.013–2.157; Ni–O(MeOH) 2.152; Ni–N, 2.035–2.088; Mg–O(ppo), 2.010–2.037; Mg–O(piv), 1.993–2.028.

There is only one coordination complex in the literature incorporating both Ni^{II} and Mg^{II}. This is the tetranuclear complex $[NiMg_3(thffo)_4Cl_4(MeOH)_4]$ (2-tetrahydrofurfuryl alcohol), where Ni and Mg are found disordered and equally distributed over the four metallic positions.[29]

$[Ni_8Sr(OH)_2(ppo)_6(piv)_{10}(Hppo)_5(Hpiv)_2(MeCN)]$ (3). The structure of **3** (Figs. 2 and 7) consists of two $[Ni^{II}_4]$ units linked together through a series of pivalate and ppo^- bridges *via* an Sr^{II} ion, which constitutes the sole link between both halfs of the cluster. The ensemble of the molecule has approximately a "U" shape, and both halves are related by a non-crystallographic two-fold axis (if the terminal ligands of one Ni^{II} ion on each side are not considered). The metals within each $[Ni^{II}_4]$ moiety are arranged as a μ_3-OH^- centered triangle, linked to a fourth further Ni^{II} center (Ni4 or Ni5) by two ppo^- and one piv^- ligand. Each of these tetranuclear fragments are attached to the central Sr^{II} ion through three pivalate and one Hppo group arising from Ni3 and Ni4, or Ni5 and Ni6, respectively.

Table 1 Crystallographic data for complexes **2**, **3** and **4**

	2	**3**	**4**
Formula	$Ni_6Mg_2O_{32}N_{19}C_{130}H_{168}$	$Ni_8SrO_{37}N_{27}C_{169}H_{205}$	$Ni_8BaO_{35.70}N_{26.75}C_{163.50}H_{197.85}$
M_r/g mol^{-1}	2909.71	3763.75	3716.06
Crystal system	Triclinic	Triclinic	Triclinic
Space group	$P\bar{1}$	$P\bar{1}$	$P\bar{1}$
a/Å	13.3879(17)	19.0435(7)	19.157(3)
b/Å	16.4548(19)	19.1516(7)	19.344(3)
c/Å	17.029(2)	30.8891(12)	30.721(4)
α/°	97.611(3)	90.0490(10)	83.202(2)
β/°	96.863(2)	96.8410(10)	89.547(2)
γ/°	103.231(3)	119.0340(10)	60.687(2)
V/Å^3	3575.8(8)	9757.4(6)	9840(3)
Z	1[b]	2	2
D_c/g cm^{-3}	1.351	1.281	1.254
T/K	100(2)	100(2)	150(2)
Crystal shape	Needle	Block	Lath
Color	Green	Green	Green
Dimensions/mm	0.40 × 0.20 × 0.20	0.30 × 0.30 × 0.20	0.12 × 0.06 × 0.03
Unique data	12422	39166	27680
Unique data with $I > 2\sigma(I)$	8080	28721	17961
R, R_w[a]	0.060, 0.161	0.059, 0.175	0.089, 0.227

[a] R, R_w are for $I > 2\sigma(I)$. $R = \Sigma||F_o| - |F_c||/\Sigma|F_o|$, $R_w = [(\Sigma w(|F_o| - |F_c|)^2/\Sigma wF_o^2)]^{1/2}$. [b] The molecule lies on an inversion center.

Table 2 Interatomic distances [Å] and angles [°] within the core of the complex $[Ni_6Mg_2(OH)_2(ppo)_4(piv)_{10}(Hppo)_4(MeOH)_2]$ (**2**)

Ni1–O1	1.997(3)	Ni1 ··· Ni2	3.3616(9)
Ni1–O7	2.204(3)	Ni3 ··· Ni2	3.454(1)
Ni1–O8	2.157(3)	Mg1 ··· Mg1′	3.160(2)
Ni3–O1	2.009(3)	Ni1–O1–Ni3	90.32(12)
Ni3–O7	2.216(3)	Ni1–O7–Ni3	79.98(10)
Ni3–O8	2.101(3)	Ni1–O8–Ni3	83.69(12)
Ni2–O1	1.985(3)	Ni1–O1–Ni2	115.18(15)
Mg1–O7	2.035(3)	Ni2–O1–Ni3	119.70(16)
Mg1–O6	2.037(3)	Ni1–O7–Mg1	106.98(13)
Mg1–O6′	2.010(3)	Ni3–O7–Mg1	106.71(14)
Ni1 ··· Ni3	2.8406(11)	Mg1–O6–Mg1′	102.66(13)

In addition to the two μ_3-hydroxides, the bridging of the metals is then insured by a total two μ_3-piv$^-$ groups (3.21 in Harris notation), two μ_2-piv$^-$ ligands (2.21), six μ-pivalates (in the *syn,syn* fashion), six ppo$^-$ moieties (four in the 3.21 and two in the 2.11 mode, respectively), and two Hppo molecules (in the 2.11 bridging mode). The latter are linking Ni3 and Ni6 to Sr, and the assigment of the charge of these two ligands has been made on the basis of the long distances from the O-donor to Sr^{II} (2.923(3) and 2.822(3) Å, respectively) and the presence of two possible hydrogen bonding interactions with the O atoms from two neighbouring ppo$^-$ groups (dashed lines in Fig. 2; O–H ··· O distances, 2.546 and 2.552 Å, respectively). The peripheral ligation of the cluster is completed by terminal ligands; there is one molecule of Hppo and one of MeCN bound to Ni1, while two monodentate Hpiv groups are attached to Ni7. These terminal ligands are the only responsible for the lack of idealized C_2 symmetry within complex **3** in the solid state. Interestingly, this asymmetry was found to be conserved on single crystals obtained from different batches and this composition was consistent with the results from microanalysis experiments performed on the bulk product. It is possible that this distribution of terminal groups is a requirement to fit the steric demands of the ligands within this arched structure

Table 3 Interatomic distances [Å] and angles [°] within the core of complexes $[Ni_8Sr(OH)_2(ppo)_6(piv)_{10}(Hppo)_5(Hpiv)_2(MeCN)]$ (**3**) and $[Ni_8Ba(OH)_2(ppo)_6(piv)_{10}(Hppo)_{5.3}(Hpiv)_{0.7}(MeCN)_2]$ (**4**), in the **3/4** format[a]

Ni1–O1	2.010(3)/2.012(6)	Ni4 ··· Ni3	3.530(1)/3.571(2)
Ni2–O1	2.046(3)/2.053(6)	Ni4 ··· Ni2	4.549(1)/4.547(2)
Ni2–O10	2.082(3)/2.096(6)	Ni4 ··· Ni1	6.832(1)/6.853(2)
Ni3–O1	2.083(3)/2.068(6)	Ni7 ··· Ni6	3.695(1)/3.685(2)
Ni3–O9	2.118(3)/2.136(6)	Ni7 ··· Ni8	3.395(1)/3.390(3)
Ni3–O10	2.030(3)/2.053(6)	Ni6 ··· Ni8	3.072(1)/3.073(2)
Ni4–O9	2.075(3)/2.094(6)	Ni5 ··· Ni6	3.526(1)/3.564(2)
Ni4–O13	2.062(3)/2.060(7)	Ni5 ··· Ni8	4.609(1)/4.571(2)
Ni4–O15	2.146(3)/2.135(7)	Ni5 ··· Ni7	6.864(1)/6.875(2)
Ni7–O27	2.007(3)/2.021(7)	M1 ··· Ni4	3.436(1)/3.564(2)
Ni6–O25	2.158(3)/2.177(6)	M1 ··· Ni5	3.432(6)/3.555(2)
Ni6–O26	2.024(3)/2.042(6)	Ni1–O1–Ni3	130.21(14)/130.5(3)
Ni6–O27	2.075(3)/2.064(7)	Ni1–O1–Ni2	113.18(13)/112.6(3)
Ni8–O26	2.084(3)/2.094(6)	Ni2–O1–Ni3	96.82(12)/97.1(3)
Ni8–O27	2.074(3)/2.069(7)	Ni2–O10–Ni3	97.35(12)/96.2(3)
Ni5–O20	2.139(3)/2.122(7)	Ni3–O9–Ni4	114.70(13)/115.3(3)
Ni5–O22	2.054(3)/2.051(7)	Ni4–O13–M1	94.63(10)/94.9(3)
Ni5–O25	2.087(3)/2.090(7)	Ni4–O15–M1	94.11(11)/94.7(3)
M1–O13	2.586(3)/2.739(7)	Ni7–O27–Ni6	129.75(15)/128.8(3)
M1–O15	2.533(3)/2.686(7)	Ni7–O27–Ni8	112.57(14)/111.9(3)
M1–O20	2.533(3)/2.665(6)	Ni8–O27–Ni6	95.52(12)/96.0(3)
M1–O22	2.596(3)/2.748(6)	Ni8–O26–Ni6	96.78(13)/95.9(3)
Ni1 ··· Ni3	3.712(1)/3.705(2)	Ni6–O25–Ni5	112.32(13)/113.2(3)
Ni1 ··· Ni2	3.386(1)/3.382(2)	Ni5–O20–M1	94.15(11)/95.2(2)
Ni2 ··· Ni3	3.088(1)/3.089(2)	Ni5–O22–M1	94.41(11)/94.5(2)

[a] M = Sr (**3**) or Ba (**4**).

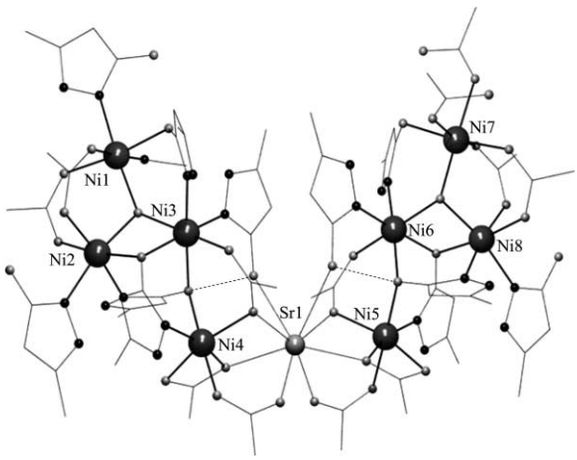

Fig. 2 Povray representation of $[Ni_8Sr(OH)_2(ppo)_6(piv)_{10}(Hppo)_5(Hpiv)_2(MeCN)]$.(**3**). Only the *ipso*-C atoms of ppo or Hppo are shown. The CH_3 groups of piv^- and hydrogen atoms have been removed for clarity. Dashed lines are H-bondings. Code for unlabelled atoms: grey, O; black, N; rest, C. Interatomic distance ranges [Å]: Ni–O(OH), 2.010–2.083; Ni–O(ppo), 2.024–2.158; Ni–O(piv), 1.997–2.146; Ni–O(Hpiv), 2.086–2.158; Ni–N(ppo or Hppo), 2.016–2.122; Ni–N(MeCN), 2.137; Sr–O(Hppo), 2.822–2.923; Sr–O(piv), 2.499–2.596.

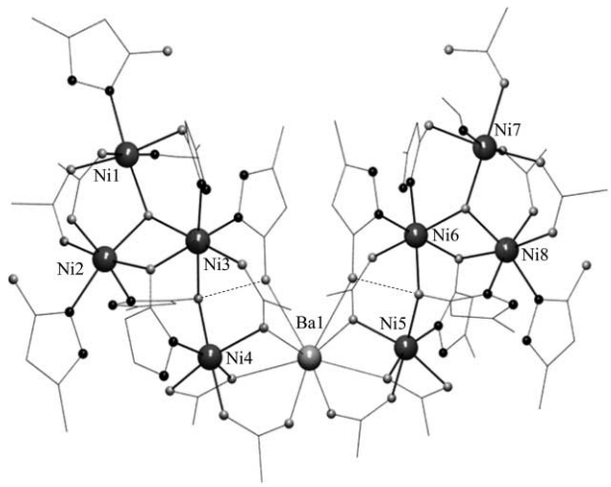

Fig. 3 Povray representation of the $[Ni_8Ba(OH)_2(ppo)_6(piv)_{10}(Hppo)_5(Hpiv)(MeCN)_2]$ component of (**4**). Only the *ipso*-C atoms of ppo or Hppo are shown. The CH_3 groups of piv^- and hydrogen atoms have been removed for clarity. Dashed lines are H-bondings. Code for unlabelled atoms: grey, O; black, N; rest, C. Interatomic distance ranges [Å]: Ni–O(OH), 2.012–2.069; Ni–O(ppo), 2.043–2.177; Ni–O(piv), 1.980–2.135; Ni–O(Hpiv), 2.107; Ni–N(ppo or Hppo), 2.020–2.130; Ni–N(MeCN), 2.120–2.128; Ba–O(Hppo), 2.914–2.987; Ba–O(piv), 2.640–2.747.

(See Fig. S1, ESI, † for a view of the structure of **3** with complete ligands). There are six types of Ni ··· Ni vectors within each $[Ni^{II}_4]$ fragment (see Table 3). These are (taking only one fragment as example); 3.386(1) (Ni1 ··· Ni2 pair), 3.712(1) (Ni1 ··· Ni3), 3.088(1) (Ni2 ··· Ni3), 3.530(1) (Ni3 ··· Ni4), 4.549(1) (Ni2 ··· Ni4), and 6.832(1) Å (Ni1 ··· Ni4), respectively. Near the link, the average Ni ··· Sr distance is 3.434 Å. The Ni^{II} centers are all in the very common distorted octahedral environment, whilst Sr^{II} has a coordination number of eight. Neither hydrogen bonding nor π–π stacking interactions were observed between clusters in the crystal. As in **2**, only C–H ··· π-ring contacts were found as cohesive force between complexes. Again, the metal centers of different clusters are well separated, with a minimum intermolecular Ni ··· Ni vector of 10.390 Å.

To the best of our knowledge, only one coordination compound combining both Ni^{II} and Sr^{II} in the structure has been reported.[30] It is a 3D coordination polymer with formula $[NiSr(C_3H_2O_4)(H_2O)_7]$ ($C_3H_2O_4H_2$ = malonic acid).

$[Ni_8Ba(OH)_2(ppo)_6(piv)_{10}(Hppo)_{5.3}(Hpiv)_{0.7}(MeCN)_2]$ (4). The structure of **4** (Fig. 3) is almost the exact Ba^{II} analogue of **3** with the exception of the terminal ligands on Ni7. In complex **4**, the terminal ligands on this metal are one molecule of MeCN and either one Hppo or one Hpiv molecule. There is positional disorder in this location, and the best refinement of the electron density map was obtained for occupancies of 70 and 30% of Hpiv and Hppo, respectively. The results from microanalysis are consistent with this assigment. In Fig. 3 is represented the major component of this solid solution, namely, that with pivalic acid on Ni7. Most of the metric parameters are very similar to these of the Sr^{II} derivative (see captions of Figs. 2 and 3 and Table 3). The most obvious differences are in the average distances of Sr/Ba to the oxygen from piv^- or Hppo. These averages differ by 0.14 (piv^-) and 0.08 (Hppo) Å. Both compounds are also similar in that there are not very significant inter-cluster interactions within the crystal. The shortest distance between Ni atoms of different clusters is 10.494 Å.

A few coordination compounds feature Ni^{II} and Ba^{II} simultaneously. These are dimeric and trimeric complexes, most of them involving macrocyclic ligands.[31–33]

Magnetochemistry

The structures of compounds **2** to **4** represent novel topologies in the area of nickel cluster chemistry. In these complexes, all Ni^{II} centers (d^8) are in a distorted octahedral environment and therefore, are presumably in a $^3A_2$ electronic state and possess a spin value of $S = 1$. This, and the possible magnetic exchange within these new molecules was investigated by bulk magnetization measurements in the three compounds.

Data for the magnetization of $[Ni_6Mg_2(OH)_2(ppo)_4(piv)_{10}(Hppo)_4(H_2O)_2]$ (**2a**) were collected from a microcrystalline sample in the 2–300 K temperature range at a constant magnetic field of 1 T. In Fig. 4 is a plot of the experimental χ_mT *vs.* T curve (where χ_m is the molar paramagnetic susceptibility corrected for the diamagnetic contribution of the sample; -1.55×10^{-3} cm^3 mol^{-1}). The value of χ_mT at room temperature is 7.98 cm^3 K mol^{-1}, slightly higher than expected for six uncoupled Ni^{II} centers with $S = 1$ and $g = 2.21$ (7.33). This value starts to increase with decreasing temperature at a rate that gets larger upon cooling. A maximum of 11.08 cm^3 K mol^{-1} is reached at 7 K, after which, a very sharp decrease is observed down to 7.70 cm^3 K mol^{-1} at 2 K. This behavior suggests the presence of ferromagnetic interactions within the cluster, leading to the population of low lying high spin multiplicity states as the temperature is lowered. The sharp decrease below 7 K could be atributed to a number of reasons; (i) the effect of ZFS, (ii) the existence of intermolecular interactions, (iii) the presence of a low-spin ground state, lying close in energy below states with larger spin numbers.

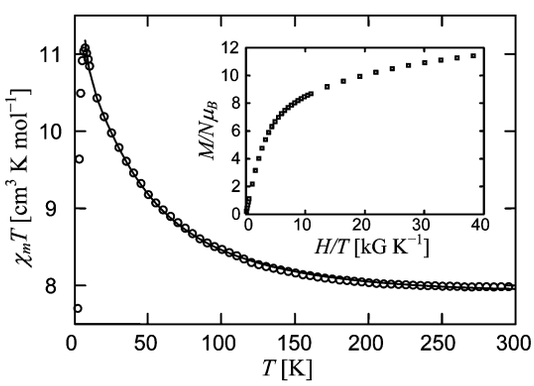

Fig. 4 Plot of experimental χ_mT *vs.* T for the complex $[Ni_6Mg_2(OH)_2(ppo)_4(piv)_{10}(Hppo)_4(MeOH)_2]$ (**2**). The solid line is a fit of the experimental data to a theoretical equation (see text for details). The inset is an isothermal $M/N\mu_B$ *vs.* H/T plot at 1.8 K.

Inspection of the structure of complex **2** (Figs. 1 and 5) allows one to interpret its magnetic behavior in terms of two independent [Ni^{II}_3] moieties. Thus, the magnetic susceptibility of the cluster could be fit to a theoretical χ_m= f(T) equation by using a model consisting of two independent isosceles triangles of Ni^{II} (S = 1). For this, it was asumed that the Ni1 ··· Ni2 and the Ni2 ··· Ni3 interactions were equivalent, differing from the Ni1 ··· Ni3 coupling. This assumption is reasonable since the Ni_{12} and Ni_{23} pairs are bridged by the same types of ligands (one μ_3-OH^- group and one μ-piv^- moiety), whereas the Ni_{23} pair is held together by one μ_3-oxygen and two μ-oxygen atoms from OH^-, ppo^- and piv^-, respectively. Also, the Ni ··· Ni distances and Ni–O–Ni angles for the first two metal pairs are very similar and distinct from these of the Ni_{23} pair (see Table 2). The Heisenberg spin-Hamiltonian arising from this model is that of eqn. (3) (corresponding to only one triangle).

$$H = -2JS_1S_3 - 2J'(S_2S_3 + S_1S_2) \quad (3)$$

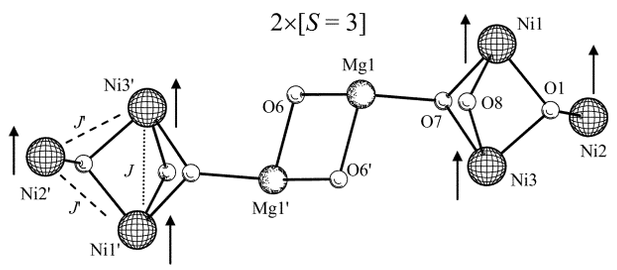

Fig. 5 Core of complex **2**, showing the spin coupling scheme between S = 1 individual moments leading to a spin ground state of two S = 3 moieties (see text for details).

As for similar systems,[34,35] the Kambe vector coupling approach can be used to transform this Hamiltonian into another, for which the eigenvalues can be found analytically (eqn. (4)).

$$E(S_T,S_A) = -J(S_A(S_A + 1) - J'[(S_T(S_T + 1) - (S_A(S_A + 1)] \quad (4)$$

This equation results from the transformations $S_A = S_1 + S_3$ and $S_T = S_A + S_2$, where $S_1 = S_2 = S_3 = 1$, with the numbering scheme as in Figs. 1 and 5. From this system arise seven different spin states with a total spin degeneracy of 27. The information about the spin states and their energy was used in the Van Vleck equation [36] which, after multiplying by two to account for both [Ni^{II}_3] fragments of the complex, was used to fit the experimental molar magnetic susceptibility. This equation does not take ZFS effects into account. A good fit of the experimental data could not be obtained when the lowest temperatures were included in the calculation, even by including a term for weak intermolecular magnetic interations using the mean field approach. This suggests that ZFS is the responsible, at least in part, for the sharp decrease of χ_mT below 7 K. Good fits could be obtained when only the data above 7 K were considered, which presumably is the range where the Van Vleck equation remains valid. The first fit was obtained with the following parameters; J = −4.8(0.2) cm^{-1}, J' = 9.9(0.5) cm^{-1}, g = 2.19(0.01) and TIP (temperature independent paramagnetism) = 1103 × 10^{-6} cm^3 mol^{-1}. These results, however, predict antiferromagnetic coupling within the Ni1 ··· Ni3 pair. This is in contradiction with previous observations [37,38] showing that for Ni–O–Ni angles below 99° (79.98–90.33° in **2**), strong ferromagnetic coupling is to be expected. However, a second set of parameters led also to a good fit of the data (Fig. 4, solid line) when the starting values of J and J' were made positive. The values of these parameters where J = 11.6(0.2) cm^{-1}, J' = 0.4(0.02) cm^{-1}, g = 2.21(0.01) and TIP = 836 × 10^{-6} cm^3 mol^{-1}. This solution is consistent with the interaction expected within the Ni1 ··· Ni3 pair. The ferromagnetic coupling manifested by this fit for the Ni_{12} and the Ni_{23} pairs is not in line with most of the cases where Ni–O–Ni angles are larger than 100° (115.18 and 119.70° in **2**). Nevertheless, the magnitude of this coupling is very small and there are examples where carboxylate-bridged Ni–(μ–O)–Ni moieties with such wide Ni–O–Ni angles display a positive J constant.[25] We therefore, consider this second solution to be the correct one, although a more detailed investigation is being conducted to confirm this end, in the context of a comprehensive study on the magnetic properties of a large family of pivalate bridged Ni^{II} clusters.

Consistent with the assigment of the spin ground state for this complex are the results from isothermal (1.8 K) magnetization measurements performed in the 0.1–70 kG field range. In Fig. 4 (inset) is a curve of the reduced magnetization ($M/N\mu_B$) per mol of **2** *vs.* H/T. The curve appears to be showing saturation towards the highest magnetic fields at a value near 12 (11.4 at 7 T), which is the expected number for a system with a ground state of S = 6 or with two S = 3 independent moieties.

The enneanuclear compounds [$Ni_8Sr(OH)_2(ppo)_6(piv)_{10}$-$(Hppo)_5(Hpiv)_2(MeCN)$] (**3**) and [$Ni_8Ba(OH)_2(ppo)_6(piv)_{10}$-$(Hppo)_{5.3}(Hpiv)_{0.7}(H_2O)_2$] (**4a**) were investigated in the same manner as complex **2**, under a constant magnetic field of 1000 G in the 2–300 K temperature range. Both clusters displayed a very similar behavior. In Fig. 6 is the plot of χ_mT *vs.* T for complex **3** after correction for the diamagnetic susceptibility, χ_{dia}, from the sample (−1.92 × 10^{-3} cm^3 mol^{-1}). The value of χ_mT at 300 K corresponds to that expected for eight magnetically uncoupled $^3A_2$ Ni^{II} centers (S = 1) per molecule, with g = 2.27 (10.36 cm^3 K mol^{-1}). It remains almost constant until a pronounced decrease starts near 100 K, falling to a value of 3.39 cm^3 K mol^{-1} at 2 K. This shows that the magnetic exchange within the cluster is dominated by antiferromagnetic interactions, but the finite value of χ_mT at the lowest measured temperature suggests that the ground state is non-diamagnetic or that the balance of anti-ferromagnetic exchange within the complicated structure is leading to population of many spin states, even at 2 K. Given the topology of the cluster, a possible ground state consists of two independent S = 2 clusters derived from ferromagnetic exchange within each hydroxide centred nickel triangle coupled anti-ferromagnetically with the fourth nickel in each arm of the "U-shaped" cluster (Fig. 7). However the measured value of χ_mT at 2 K is well below that calculated for two S = 2 states (7.26 cm^3 K mol^{-1} for g = 2.2), suggesting this picture is simplistic. If we include weak anti-ferromagnetic exchange between the S = 2 units, this could explain why the measured value is low.

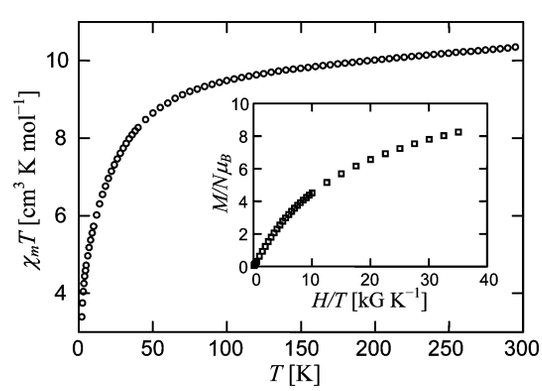

Fig. 6 Plot of experimental χ_mT *vs.* T for the complex [$Ni_8Sr(OH)_2$-$(ppo)_6(piv)_{10}(Hppo)_5(Hpiv)_2(MeCN)$] (**3**). The inset is an isothermal $M/N\mu_B$ *vs.* H/T plot at 1.8 K.

Magnetisation studies do not help (inset Fig. 6), with a behaviour that does not clearly indicate a precise spin ground state, probably because excited states of higher spin multiplicity than the ground state become populated as the magnetic field is increased. Saturation is not achieved, although it appears that a plateau at around 8 μ_B is being reached at the highest measured

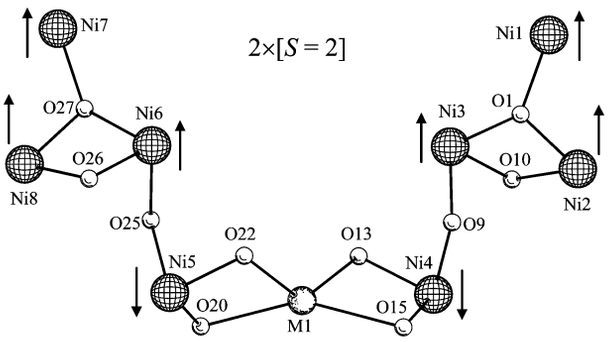

Fig. 7 Core of complexes **3** and **4**, showing the spin coupling scheme $S = 1$ individual moments leading to the postulated spin ground state of two $S = 2$ moieties (see text for details). M1 = Sr1 and Ba1 for **3** and **4**, respectively.

field. This value would be consistent with a spin ground state of $S = 4$, but this is could only be the ground state in a field of 7 T. Similar problems have been found in other nickel cages.[39] Further studies are necessary to give a precise value to the spin ground state in **3**. The behaviour of complex **4a** (not shown) is similar to that of **3**, with $\chi_m T$ values of 11.00 cm^3 K mol^{-1} at 300 K and of 3.24 cm^3 K mol^{-1} at 2 K, using a correction of $\chi_{dia} = -1.82 \times 10^{-3}$ cm^3 mol^{-1}.

Conclusions

In this report, it has been shown that changing the nature of the alkaline-earth M^{II} metal of an added base can be used synthetically to create new topologies in Ni^{II} cluster chemistry, as has been previously seen with Group 1 ions. Thus, three polynuclear Ni^{II}/piv$^-$ complexes showing two distinct structural types have been prepared and crystallographically characterized, incorporating Mg^{II}, Sr^{II} or Ba^{II}, namely $[Ni_6Mg_2(OH)_2(ppo)_4(piv)_{10}(Hppo)_4(MeOH)_2]$ (**2**), $[Ni_8Sr(OH)_2(ppo)_6(piv)_{10}(Hppo)_5(Hpiv)_2(MeCN)]$ (**3**) and $[Ni_8Ba(OH)_2(ppo)_6(piv)_{10}(Hppo)_{5.3}(Hpiv)_{0.7}(MeCN)_2]$ (**4**). The topologies of these complexes are unprecedented and all of them show two bridged and magnetically coupled $[Ni^{II}_x]$ (x = 3 or 4) moieties, structurally linked within the same molecule by two Mg^{II} or one M^{II} center (M = Sr or Ba), which maintain them magnetically independent. The results from bulk magnetization measurements strongly suggest that the $[Ni_6Mg_2]$ cluster consists of two independent fragments, each in the $S = 3$ spin ground state. On the other hand, both $[Ni_8M]$ (M = Sr and Ba) aggregates display the same magnetic behavior and, at the current stage of the investigation, two independent $S = 2$ moieties are invoked to interpret the magnetic susceptibility and magnetization measurements.

The results reported here and in a previous paper underscore the fact that in the aproach of "serendipitous assembly" for preparing new 3d shell high-spin molecules, the effect of the numerous variables in a reaction system can be traced individually and exploited effectively in the production of families of new clusters with a variety of structures.

References

1 R. E. P. Winpenny, *Adv. Inorg. Chem.*, 2001, **52**, 1.
2 A. J. Blake, C. M. Grant, S. Parsons, J. M. Rawson and R. E. P. Winpenny, *J. Chem. Soc., Chem. Commun.*, 1994, 2363.
3 A. K. Powell, S. L. Heath, D. Gatteschi, L. Pardi, R. Sessoli, G. Spina, F. Delgiallo and F. Pieralli, *J. Am. Chem. Soc.*, 1995, **117**, 2491.
4 G. Aromí, M. J. Knapp, J. P. Claude, J. C. Huffman, D. N. Hendrickson and G. Christou, *J. Am. Chem. Soc.*, 1999, **121**, 5489.
5 E. K. Brechin, C. Boskovic, W. Wernsdorfer, J. Yoo, A. Yamaguchi, E. C. Sañudo, T. R. Concolino, A. L. Rheingold, H. Ishimoto, D. N. Hendrickson and G. Christou, *J. Am. Chem. Soc.*, 2002, **124**, 9710.
6 O. Kahn, *Magnetism: A Supramolecular Function*, Kluwer Academic Publishers, Dordrecht, 1996.
7 R. Sessoli, D. Gatteschi, A. Caneschi and M. A. Novak, *Nature*, 1993, **365**, 141.
8 G. Christou, D. Gatteschi, D. N. Hendrickson and R. Sessoli, *MRS Bull.*, 2000, **25**, 66.
9 D. Gatteschi and R. Sessoli, *Angew. Chem., Int. Ed.*, 2003, **42**, 268.
10 V. Marvaud, J. M. Herrera, T. Barilero, F. Tuyeras, R. Garde, A. Scuiller, C. Decroix, M. Cantuel and C. Desplanches, *Monatsh. Chem.*, 2003, **134**, 149.
11 G. Aromí, P. Gamez, O. Roubeau, H. Kooijman, A. L. Spek, W. L. Driessen and J. Reedijk, *Angew. Chem., Int. Ed.*, 2002, **41**, 1168.
12 L. K. Thompson, L. Zhao, Z. Q. Xu, D. O. Miller and W. M. Reiff, *Inorg. Chem.*, 2003, **42**, 128.
13 G. Aromí, S. M. J. Aubin, M. A. Bolcar, G. Christou, H. J. Eppley, K. Folting, D. N. Hendrickson, J. C. Huffman, R. C. Squire, H. L. Tsai, S. Wang and M. W. Wemple, *Polyhedron*, 1998, **17**, 3005.
14 R. E. P. Winpenny, *Comments Inorg. Chem.*, 1999, **20**, 233.
15 C. Cadiou, R. A. Coxall, A. Graham, A. Harrison, M. Helliwell, S. Parsons and R. E. P. Winpenny, *Chem. Commun.*, 2002, 1106.
16 D. J. Price, S. R. Batten, B. Moubaraki and K. S. Murray, *Chem. Commun.*, 2002, 762.
17 M. Murrie, D. Biner, H. Stoeckli-Evans and H. U. Güdel, *Chem. Commun.*, 2003, 230.
18 E. K. Brechin, R. A. Coxall, A. Parkin, S. Parsons, P. A. Tasker and R. E. P. Winpenny, *Angew. Chem., Int. Ed.*, 2001, **40**, 2700.
19 E. Diamantopoulou, C. P. Raptopoulou, A. Terzis, V. Tangoulis and S. P. Perlepes, *Polyhedron*, 2002, **21**, 2117.
20 L. F. Jones, E. K. Brechin, D. Collison, A. Harrison, S. J. Teat and W. Wernsdorfer, *Chem. Commun.*, 2002, 2974.
21 A. L. Dearden, S. Parsons and R. E. P. Winpenny, *Angew. Chem., Int. Ed.*, 2001, **40**, 151.
22 G. Aromí, A. Bell, S. J. Teat, A. G. Whittaker and R. E. P. Winpenny, *Chem. Commun.*, 2002, 1896.
23 C. J. Milios, E. Kefalloniti, C. P. Raptopoulou, A. Terzis, R. Vicente, N. Lalioti, A. Escuer and S. P. Perlepes, *Chem. Commun.*, 2003, 819.
24 G. Aromí, A. R. Bell, M. Helliwell, J. Raftery, S. J. Teat, G. A. Timco, O. Roubeau and R. E. P. Winpenny, *Chem., Eur. J.*, 2003, **9**, 3024.
25 H. Andres, G. Chaboussant, H.-U. Güdel, E. J. L. McInnes, A. Parkin, S. Parsons, G. Rajaraman, A. A. Smith, G. A. Timco and R. E. P. Winpenny, *Chem., Eur. J.*, submitted.
26 In SHELX-PC Package, Madison, WI, 1998.
27 Harris notation describes the binding mode as $[X.Y_1Y_2Y_3 \cdots Y_n]$, where X is the overall number of metals bound by the whole ligand, and each value of Y refers to the number of metal atoms attached to the different donor atoms. Therefore for fpo, there will be two values for Y. The ordering of Y is listed by the Cahn–Ingold–Prelog priority rules, hence O before N. See: R. A. Coxall, S. G. Harris, D. K. Henderson, S. Parsons, P. A. Tasker and R. E. P. Winpenny, *J. Chem. Soc., Dalton Trans.*, 2000, 2349.
28 A. W. R. Addison, T. N. Rao, J. Reedijk, J. v Rijn and G. C. Verschoor, *J. Chem. Soc., Dalton Trans.*, 1984, 1349.
29 Z. Janas, L. B. Jerzykiewicz, P. Sobota and J. Utko, *New J. Chem.*, 1999, **23**, 185.
30 I. G. de Muro, M. Insausti, L. Lezama, J. L. Pizarro, M. I. Arriortua and T. Rojo, *Eur. J. Inorg. Chem.*, 1999, 935.
31 F. Vanveggel, S. Harkema, M. Bos, W. Verboom, C. J. Vanstaveren, G. J. Gerritsma and D. N. Reinhoudt, *Inorg. Chem.*, 1989, **28**, 1133.
32 F. Vanveggel, M. Bos, S. Harkema, H. Vandebovenkamp, W. Verboom, J. Reedijk and D. N. Reinhoudt, *J. Org. Chem.*, 1991, **56**, 225.
33 L. Carbonaro, M. Isola, P. La Pegna, L. Senatore and F. Marchetti, *Inorg. Chem.*, 1999, **38**, 5519.
34 A. Escuer, R. Vicente, S. B. Kumar, X. Solans, M. FontBardia and A. Caneschi, *Inorg. Chem.*, 1996, **35**, 3094.
35 S. Bhaduri, M. Pink and G. Christou, *Chem. Commun.*, 2002, 2352.
36 J. H. Van Vleck, *The Theory of Electric and Magnetic Susceptibilities*, Oxford Univesity Press, 1932.
37 M. A. Halcrow, J. S. Sun, J. C. Huffman and G. Christou, *Inorg. Chem.*, 1995, **34**, 4167.
38 J. M. Clemente-Juan, B. Chansou, B. Donnadieu and J. P. Tuchagues, *Inorg. Chem.*, 2000, **39**, 5515.
39 M. Murrie, H. Stoeckli-Evans and H. U. Güdel, *Angew. Chem., Int. Ed.*, 2001, **40**, 1957.